

Concentration and Molecular Weight Dependence of the Quenching of Ru(bpy)₃²⁺ by Ferricyanide in Aqueous Solutions of Synthetic Hyaluronan

Thomas Kluge, Akiko Masuda, Koichi Yamashita, and Kiminori Ushida*

RIKEN (The Institute of Physical and Chemical Research), Wako, Saitama, 351-0198, Japan

Received April 26, 1999; Revised Manuscript Received November 22, 1999

ABSTRACT: The quenching of electronically excited Ru(bpy)₃²⁺ (bpy = 2,2'-bipyridine) by ferricyanide (FC) in highly viscous aqueous solutions of synthetic hyaluronan (HA) was studied. The quenching reaction was found to occur by direct electron transfer at short times and by diffusional encounter at longer times after the excitation flash. Intrinsic and diffusional quenching rate constants were found to decrease with increasing polymer concentration but not with increasing molecular weight of HA, although the effect of both parameters on macroscopic viscosity was comparable. It was also found, that the lifetime of the sensitizer increased with increasing polymer concentration, indicating retarded quenching by oxygen. Efficient diffusion of the reactants in the aqueous pseudophase occurs even in solutions with high macroscopic viscosity. We compared two kinds of HAs (biosynthetic and animal source) in the present experiments and obtained a sharp contrast in photochemical properties between them while other observable macroscopic parameters showed no difference. Biosynthetic HA is more suitable for the systematic study to elucidate the molecular weight dependence of the present photochemical properties showing microscopic aspects of the HA solution.

Introduction

Hyaluronan (HA) is a high molecular weight biopoly-saccharide of the glucosaminoglycan family. The repeating unit is 2-acetamido-2-deoxy-3-*O*-(β -D-glucopyranosyluronic acid)- β -D-glycopyranoside. HA occurs in many living substrates such as the extracellular matrix and synovial fluids and acts as a lubricant and shock absorber. Its hydrodynamic behavior is quite unique among polymer solutions. Even at fairly low concentration, it forms highly viscous aqueous solutions. The conformation of the HA chains has been studied for some time using a couple of methods including NMR,^{1,2} Raman, and infrared spectroscopy,³ electron microscopy,^{4,5} neutron and X-ray scattering,⁶ vacuum ultraviolet circular dichroism,⁷ and computer simulation.⁸ Large network structures have been found to determine its viscoelastic behavior. In the case of higher molecular weight HA, dilute, semidilute, and concentrated regions can be distinguished.⁹ They differ mainly in the degree of chain overlap and segment distribution. An important parameter for the characterization of HA solutions is the specific viscosity. It has been found that its value increases with both molecular weight and concentration of the polymer.^{10,11} In addition to that, the viscosity can be altered by changing the pH and the ionic strength of the solution. A comprehensive review on the properties of HA has been published recently.¹²

Despite these rheologic properties, the diffusion of small molecules such as urea, sugars, and proteins is still relatively fast. This combination of mechanical stability and effective reactant transportation is the key element for the biological functionality of HA. Together with its biocompatibility, it is an interesting target molecule for pharmaceutical research. The biological effectiveness of many drugs, free radicals, hormones, and other physiologically active molecules is determined by their mobility in HA solutions. Therefore, information about reactant transport is highly required, to understand and control such important processes as drug

release and diseases caused by HA degradation. Photochemical processes are an ideal tool for this task, because they can be initiated and followed in situ very easily.

As a model reaction, we chose the well-characterized electron-transfer quenching reaction between Ru(bpy)₃²⁺ (bpy = 2,2'-bipyridine), which will be denoted by Rubpy hereafter, and ferricyanide (FC), which has been used previously in the study of polymer solutions.¹³ In a preliminary communication, we reported that the diffusion of the negatively charged FC ion is hindered in concentrated solutions of animal HA. It was found that the parameters describing the fluorescence decay change with structural changes in the polymer solution.¹⁴

In this work, we studied the influence of concentration and molecular weight of synthetic HA on the quenching of excited Rubpy by FC in aqueous solution. It is known that synthetic and bacterial HA samples differ from those derived from animal sources due to the higher content of proteins in the latter.¹⁵ These proteins are known to enhance chain entanglement and therefore alter both structure and rheologic behavior of HA solutions. Especially from the viewpoint of biocompatibility, the study of synthetic samples is very important. By analyzing the fluorescence decay of the excited Rubpy in different HA solutions, quenching rate constants were obtained. In combination with viscosity measurements, their dependence on concentration and molecular weight of the polymer is explained on the basis of structural changes in the corresponding HA solutions.

Experimental Section

Four different samples of HA were used within this work. Cocks comb HA was obtained from TCI (Tokyo). It will further be referred to as HACC. Three synthetic HA samples with labeled molecular weights 300 000 (HAM0.3), 1 000 000 (HAM1) and 2 000 000 (HAM2) were obtained from Denki Kagaku

Kogyo Co., Ltd. Their molecular weights are controlled on the first biosynthesis step. Ru(bpy)₃Cl₂·6H₂O (Aldrich) and K₃[Fe(CN)₆] (Wako Chemicals, Tokyo) were used as received. The HA solutions were prepared by stirring the polymer in an isotonic solution of Na₂HPO₄/KH₂PO₄ buffer (pH 7.0) containing the sensitizer (5×10^{-5} M, calculated from 452 nm absorption using $\epsilon = 14\,400\text{ cm}^{-1}$) until a homogeneous solution was obtained. Stirring times varied between 2 and 12 h, dependent on the sample volume. For the quenching experiments, suitable amounts of a concentrated stock solution of the quencher were added to the HA sample.

All molecular weight data of the HA samples were obtained by gel filtration chromatography (GFC) at 30 °C, using a Millennium 486 systems (Waters) and a refractive index detector with a OHpak SB-806 HQ column (Shodex). An aqueous solution of 0.1 M NaNO₃ was used as eluent at flow rate of 1.0 mL min⁻¹, and a sample concentration of 0.5 mg mL⁻¹ was applied. Poly(ethylene oxide) with a low polydispersity was used as a standard to calibrate chromatograms. Number-average molecular weight (M_n), weight-average molecular weight (M_w), and polydispersity (M_w/M_n) of the HA samples were calculated from the GFC data. The obtained values of M_w/M_n were 1890K/897K = 2.10 (HACC), 1010K/426K = 2.37 (HAM0.3), 3050K/1280K = 2.38 (HAM1) and 4890K/2650K = 1.85 (HAM2). Experimentally obtained M_n for synthetic samples about 3–40% exceeds the labeled values.

Fluorescence decay curves were measured using a conventional single-photon counting apparatus (Horiba NAES 1100). A hydrogen-filled flash lamp having about 4 ns pulse duration (full width at half-maximum) was used as the excitation source. The samples were excited in the wavelength region from 420 to 480 nm using the combination of a cutoff and a band-pass filter. The emission was accumulated using a 570 nm cutoff filter. All samples were air-saturated.

The luminescence decay profiles were analyzed with non-linear least-squares fits using standard criteria, i.e., distribution of the residuals, autocorrelation function of the residuals, and χ^2 values. An iterative reconvolution method with the respective decay model and the simultaneously measured decay function of the flash lamp was used to obtain the decay parameters.

Viscosity measurements were carried out using a model DV-III cone/plate viscometer (Brookfield Engineering Labs., Inc.) with a CPE-51 cone. By using this setup, the shear rates can be varied between 0 and 768 s⁻¹. The measurable viscosity range is 25.6–512 000 mPa s.

All measurements were performed at 298 K.

Results

Viscosity Measurements. HA behaves as a non-Newtonian fluid and shows shear thinning over a wide range of shear rates and concentrations. This effect is due to alignment of the chains under the influence of shear stress resulting in a decrease in the macroscopic viscosity. To characterize the HA solutions used in the quenching experiments, simultaneous measurements of the shear rate dependence of the macroviscosity were done. The small sample volume required for these measurements (0.5 mL) allowed us to directly measure the viscosity of the samples used in the quenching experiments. This ensures that in all cases the viscosity under the conditions of the corresponding quenching experiment is obtained.

For the analysis of the recorded viscosity vs shear rate curves, we used an equation proposed earlier^{16,17} for the determination of the viscosity parameters of a wormlike polyelectrolyte

$$\eta = \frac{\eta_0}{\left(1 + \left(\frac{\gamma}{\gamma_{0.5}}\right)^n\right)} \quad (1)$$

Table 1. Zero-Shear Viscosity^a η_0 and Exponent^b n for Different Concentrations and Molecular Weights of HA

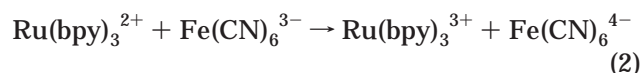
| c/wt % | HAM0.3 | | HAM1 | | HAM2 | |
|--------|-----------------|------|-----------------|------|-----------------|------|
| | η_0 /mPa s | n | η_0 /mPa s | n | η_0 /mPa s | n |
| 0.5 | <3 | | <3 | | 860 | 0.72 |
| 0.8 | <3 | | 870 | 0.72 | 8200 | 0.77 |
| 1.0 | 70 | 0.85 | 3100 | 0.76 | 29000 | 0.83 |
| 1.2 | 140 | 0.84 | 5300 | 0.78 | 57000 | 0.84 |
| 1.5 | 240 | 0.77 | 14000 | 0.82 | 260000 | 0.78 |
| 2.0 | 790 | 0.78 | 74000 | 0.75 | | |
| 3.0 | 4300 | 0.85 | | | | |

^a Estimated errors about 10%. ^b Estimated errors about 0.05.

where η_0 is the zero shear viscosity and γ is the shear rate. The magnitude of η decreases with increase of the shear rate, and $\gamma_{0.5}$ is defined as the shear rate at which the viscosity is reduced to $\eta_0/2$.

According to eq 1, a linear plot of $\eta\gamma^n$ against η is expected. In the work mentioned above, a value of 0.76 for n was suggested. However, in our experiment this value sometimes led to a poor correlation. Therefore, we varied the exponent in order to obtain a good linear fit. By this method, slightly different values for n were obtained (Table 1). Because of the lack of any systematic change with either molecular weight or concentration of the polymer, this variation is likely due to experimental errors. The average value agrees satisfactorily with the value suggested in previous studies. The zero-shear viscosity η_0 for different HA solutions studied in this work (containing the reactants, Rubpy and FC) are also given in Table 1. In agreement with previous studies,⁹ they were found to increase with both concentration and molecular weight of the polymer. By adjusting both factors, the macroviscosity of the solution was varied over 5 orders of magnitude.

Fluorescence Measurements. To study the effects of concentration and molecular weight of synthetic HA on the transport and reaction behavior of reactants in aqueous solution, we choose the model system (2). The



excited state of the sensitizer Ru(bpy)₃²⁺ formed by excitation into its metal-to-ligand charge transfer (MLCT) band is oxidatively quenched by FC according to an electron-transfer mechanism. This reaction has been followed by measuring the emission decay curves of the sensitizer in dependence on the quencher concentration. In the absence of quencher molecules, the decay of the sensitizer was single exponential at least over a period of four lifetimes (Figure 1, curve a). The lifetimes obtained for different HA solutions are given in Table 2. They were found to increase with increasing concentration of the polymer. In contrast, almost no dependence of the lifetime of Rubpy on the molecular weight of the polymer was found. In reference to the macroviscosity in Table 1, there is no overall correlation between this parameter and the lifetime of the sensitizer. In addition, no apparent spectral shift with the existence of HA was observed in either absorption and emission measurements, while Coulomb interaction between positive charged Rubpy and anionic HA chain is expected. Our previous study¹⁴ with methyl viologen (MV²⁺) as the quencher in HA solution showed that the electron-transfer reaction between these two positive ions (Rubpy and MV²⁺) was a normal diffusion-con-

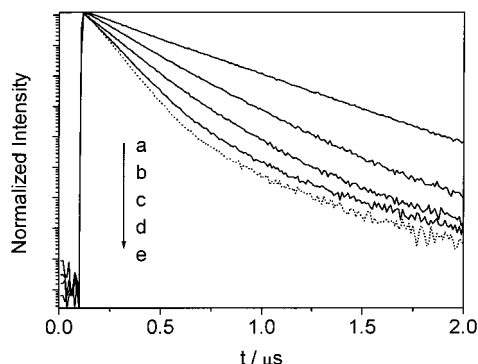


Figure 1. Fluorescence decay curves (logarithmic scale) of Rubpy. From top to bottom the curves are as follows: (a–d) Rubpy in 1.5 wt % HAM2 with 0, 0.22, 0.44, and 0.65 mM FC, respectively; (e) Rubpy in water with 0.65 mM FC (dashed line). All these curves are normalized at the maximum points of each decay.

Table 2. Lifetimes^a τ_0 in ns of Ru(bpy)₃²⁺ for Different Concentrations and Molecular Weights of HA

| c/wt % | HAM0.3 | HAM1 | HAM2 |
|--------|--------|------|------|
| 0 | 385 | 385 | 385 |
| 0.5 | 392 | 407 | 402 |
| 0.8 | 402 | 417 | 418 |
| 1.0 | 418 | 422 | 427 |
| 1.2 | 431 | 430 | 430 |
| 1.5 | 448 | 434 | 429 |
| 2.0 | 448 | | |

^a Estimated errors about 5%.

trolled one. Its rate constant was almost equal to that observed without HA. Therefore, we believe that Rubpy (and also MV²⁺) can travel freely inside the HA solution.

In the presence of the quencher FC, nonexponential decay curves for the fluorescence of the sensitizer Rubpy were obtained both in water and in HA solution (Figure 1). As described in our previous work,¹⁴ static quenching originating from ion pairs between Rubpy and FC causes a decrease in the luminescence intensity at $t = 0$. Since we only discuss the quenching time profiles especially after a long time delay, all the curves are normalized at their maximum intensities. In the same paper,¹⁴ we used the Infelta–Tachiya model^{18–20} to describe the decay function. Although this model successfully fitted the experimental data, this does not prove its applicability for our system. In particular, the assumption of an independent Poisson distribution of the reactants, made in this model, might be critical because of their rather high charge. In this work, we use a more general approach, which will be described in the following section.

The fluorescence decay function of an excited sensitizer in the presence of quencher molecules in the absence of static quenching and in the case that the quenching constants do not vary with time can be described by eq 3,¹⁴ where I_0 , τ_0 , $[Q]$ and k_q are the

$$I(t) = I_0 \exp\left(-\frac{t}{\tau_0} - [Q]k_q t\right) \quad (3)$$

fluorescence intensity of the sensitizer at time zero, the fluorescence lifetime of the sensitizer in a quencher-free solution, the quencher concentration, and the quenching rate constant, respectively. The other symbols have their usual meanings. According to eq 3, the quenching rate

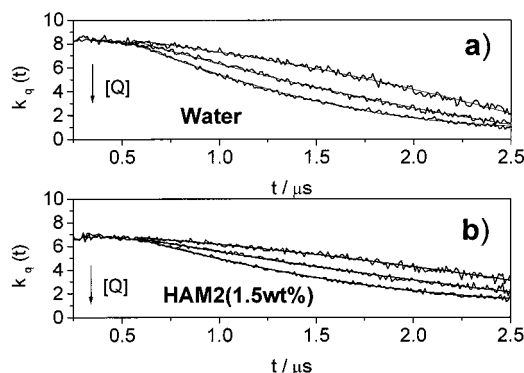


Figure 2. Time dependence of the quenching rate constants, calculated using eq 4 for the quencher concentrations 0.22, 0.44, and 0.65 mM (from top to bottom), respectively, for (a) water and (b) 1.5 wt % HAM2. The straight lines represent the fit to eq 5 at longer times.

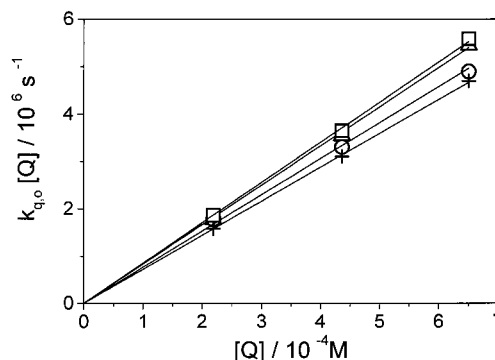


Figure 3. Values of $k_{q,0}[Q]$ vs quencher concentration for 5×10^{-5} M Ru(bpy)₃²⁺ in isotonic buffer solution (square) and 0.5 wt % (triangle), 0.8 wt % (circle), and 1.5 wt % (cross) solutions of HAM2.

constant can be obtained from the measured fluorescence decay curves in the presence ($I_q(t)$) and absence ($I_0(t)$) of the quencher by using eq 4. Typical curves for

$$k_q = \frac{1}{[Q]t} \ln\left(\frac{I_0(t)}{I_q(t)}\right) \quad (4)$$

k_q in dependence of time are shown in Figure 2. It is obvious that the condition of time-independent quenching rate constants is only fulfilled at short times up to about 500 ns after the excitation flash. To obtain the quenching constants in this time region, an iterative reconvolution algorithm according to eq 5 with the

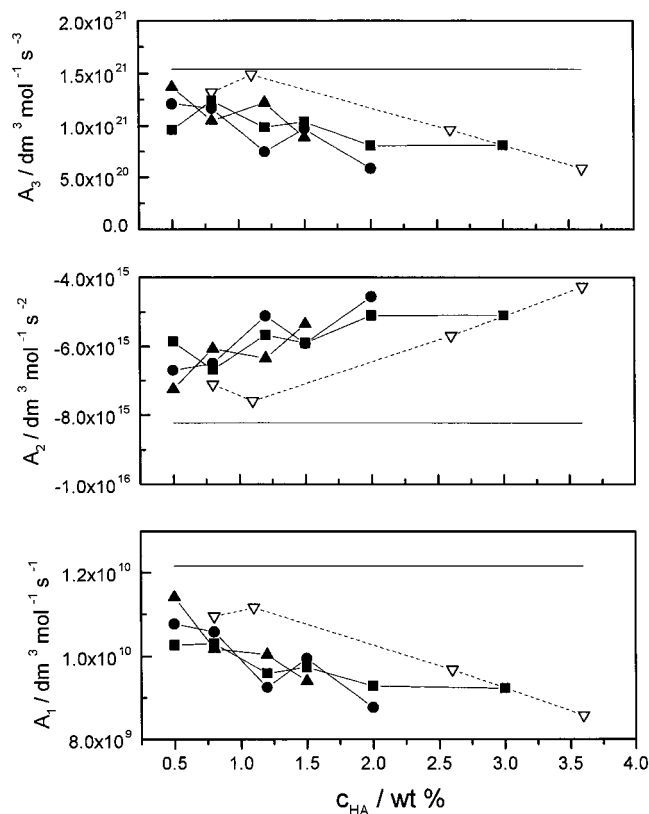
$$F_i = A \left[\sum_{j=1}^i G_j I(t_i - t_j) \right] \quad (5)$$

model given by eq 3 was performed, where F and G are the measured probe and lamp decay functions, respectively.

The parameters were the initial fluorescence intensity I_0 , the rate of the fluorescence decay in quencher-free solution, which was obtained from independent experiments and kept constant in the fitting procedure, and $[Q]k_{q,0}$, where $k_{q,0}$ is the intrinsic quenching rate constant. As expected, the last parameter varied linearly with quencher concentration, as shown in Figure 3. The rate constants obtained by this method are given in Table 3.

Table 3. Intrinsic Bimolecular Quenching Rate Constants^a $k_{q,0}$ (mol dm⁻³s⁻¹)

| <i>c</i> /wt % | HAM0.3 | HAM1 | HAM2 |
|----------------|-------------------|-------------------|-------------------|
| 0 | 8.5×10^9 | 8.5×10^9 | 8.5×10^9 |
| 0.5 | 8.2×10^9 | 8.1×10^9 | 8.3×10^9 |
| 0.8 | 7.8×10^9 | 7.7×10^9 | 7.6×10^9 |
| 1.2 | 7.5×10^9 | 7.5×10^9 | 7.5×10^9 |
| 1.5 | 7.6×10^9 | 7.4×10^9 | 7.2×10^9 |
| 2.0 | 6.9×10^9 | 6.6×10^9 | |
| 3.0 | 6.7×10^9 | | |

^a Estimated errors about 5%.**Figure 4.** Change of the parameters, obtained by fitting of the time-dependent rate constants, calculated from eq 4, to eq 5 with increasing HA concentration for HAM0.3 (black square), HAM1 (black circle), HAM2 (black up triangle), and HACC (white down triangle, broken line). The horizontal line denotes the value, obtained in buffer solution.

At longer time scales a rapid decrease of k_q with time was found, which can be described by a polynomial model for $k_q(t)$.

$$k_q(t) = A_1 + A_2 t + A_3 t^2 \quad (6)$$

The values of the parameters A_{1-3} were found to vary linearly with quencher concentration. Their values for the highest quencher concentration are given in Figure 4 for HA solutions of different concentration and molecular weight. Lower concentrations yield similar curves. Polynomial models similar to eq 6 were found previously for quenching processes, occurring by random walk of the quencher molecules in both Euclidean and fractal dimensions.^{13,21-23} Within the framework of this theory, a reaction zone surrounding each excited sensitizer molecule may be defined, in which distant dependent direct electron transfer is feasible. The corresponding rate constant (in a simplified form) is given by eq 7, where a is the distance of closest approach

$$k(r) = k(a) \exp(-\beta[r - a]) \quad (7)$$

of the reactants and β is a constant, describing the decrease of the rate constant with distance. As shown previously, this model yields for short-ranged interactions with exponential distance dependence an exponential decay function at short times. This is in agreement with the behavior found for the decay of excited Rubpy in the presence of FC at times shorter than 500 ns. In the case of rather high quencher concentrations, each excited Rubpy has a quencher molecule in the reaction zone, leading to a single-exponential decay for all times. However, if the quencher concentration is low, as in our case, a certain number of excited sensitizer molecules do not have a quencher molecule nearby. These molecules are quenched by a migration mechanism, involving the diffusion of a quencher molecule by random walk, until it reaches the reaction zone, where it quenches the sensitizer with a rate corresponding to eq 7. Therefore, with time the quenching mechanism changes from reaction-controlled to diffusion-controlled. The rate constants for the diffusion-controlled process can be obtained by relating the parameters of the polynomial fit (eq 6) to the theory of quenching by random walk of the quencher molecules in restricted geometries. Within the framework of this theory, using a cumulant expansion of the survival probability of the random walker, the following decay law is predicted for long times

$$I(t) \approx \exp \sum_{i=1}^{\infty} \kappa_i(t) \frac{(-\lambda)^i}{i!} \quad (8)$$

where $\kappa_i(t)$ are the cumulants and $\lambda = -\ln(1-p)$, with the occupation probability p . Comparing eq 8 with eq 6, the first, second, and third terms of the sum in eq 8 can be assigned to A_1 , A_2 , and A_3 , respectively. Because the reaction rate at long times is controlled by the diffusion into the reaction zone, the first two cumulants $\kappa_1(t)$ and $\kappa_2(t)$ can be interpreted as the mean and the variance of the diffusion rate constant, respectively.¹³ The third cumulant, also used in the fitting, is a rather complicated expression, which also depends on the diffusion rate. A similar model, without the direct transfer contribution, has been applied successfully to the description of the fluorescence decay of excited Rubpy quenched by FC in polymer solutions.¹³ In that work, eq 6 was extended to arbitrary dimensions of the reaction space by introducing the fractal dimension f into the exponent of the time series, leading to eq 9. In

$$k_q(t) = A_1 t^{f-1} + A_2 t^{2f-1} + A_3 t^{3f-1} \quad (9)$$

our case, fitting of the experimental decay curves to eq 9 always gave values for f which were very close to 1. In this case, eq 9 goes over into eq 6. This result indicates that the quenching reaction occurs in the classical region of the kinetic phase diagram.²⁴

Discussion

Viscosity Measurements. In agreement with earlier studies,⁹ the zero shear rate viscosity was found to increase with both concentration and molecular weight of HA. Usually, a power law is applied to describe the dependence of η_0 on polymer concentration

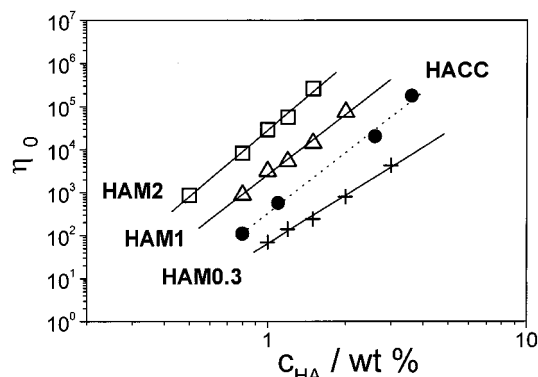


Figure 5. Variation of η_0 with concentration for HA of different molecular weight for HAM0.3 (cross), HACC (black circle, dashed line), HAM1 (white triangle), and HAM2 (white square), in the order from the bottom of figure with fitted lines $\propto c^{3.7}$, $c^{4.7}$, $c^{4.7}$, and $c^{5.1}$, respectively.

$$\eta_0 \propto c^y \quad (10)$$

where c is the concentration of HA in wt %. Therefore, a double-logarithmic plot of η_0 vs c should be linear, as shown in Figure 5. Using the data in Table 1, values of 3.7, 4.7, and 5.1 were found for y in the case of HAM0.3, HAM1, and HAM2, respectively. In the paper mentioned above, almost no variation of the exponent was found in bacterial HA of similar molecular weight. Average values of 1.2 and 4.0 were reported for y in the dilute and concentrated region, respectively. Comparison with the values above indicate that our experiments were carried out in the concentrated region. This assignment is further justified by the molecular weight dependence of the zero shear viscosity, which can also be expressed by an exponential law (eq 11). When the number-

$$\eta_0 \propto M^z \quad (11)$$

average molecular weight (M_n) in the present results is used, the average variation with M was found to be proportional to $M^{3.3}$. This dependence is slightly weaker than the value found for bacterial HA in the concentrated region ($z = 4$), but considerably stronger than the value in dilute solution ($z = 1$). It also indicates a slightly more pronounced dependence of the viscosity on concentration compared to molecular weight.

The dependence of the zero shear rate viscosity on the concentration of HACC was also studied. The values for HACC sample solutions containing Rnbpy and FC are given in Table 4 and the plot is also shown in Figure 5 with a dashed line. They were found to be proportional to $c^{4.7}$, which is close to the cases of HAM1 and HAM2. The dashed line locates between the lines for HAM0.3 and HAM1 reasonably in the order of their M_w .

No clear trend could be found in the case of the exponent n (eq 1, Tables 1 and 4). This is likely due to the uncertainty introduced by the method of its determination.

The effect of the reactants on the viscosity of synthetic HA was also studied. The result is shown in Figure 6. By adding Rubpy and FC to the HA solution, the variation of η_0 with molecular weight changes from a $M^{4.4}$ -law to a $M^{3.3}$ -law. The first one is close to the behavior found previously for HA from bacterial sources, whereas the latter one is typical for flexible polymers. This indicates that the addition of Ru(bpy)₃²⁺ and Fe(CN)₆³⁻ leads to decreasing stiffness of the HA chain.

Table 4. Viscosity Parameters and Intrinsic Quenching Rate Constants in HACC

| $c/\text{wt } \%$ | HACC | | $k_{q,0}^c/10^9$ $\text{mol dm}^{-3} \text{ s}^{-1}$ |
|-------------------|-------------------------|-------|---|
| | $\eta_0/\text{mPa s}^a$ | n^b | |
| 0.8 | 110 | 0.75 | 8.0 |
| 1.1 | 570 | 0.70 | 8.2 |
| 2.6 | 20200 | 0.77 | 7.6 |
| 3.6 | 178000 | 0.60 | 6.4 |

^a Estimated errors about 10%. ^b Estimated errors about 0.05. ^c Estimated errors about 5%.

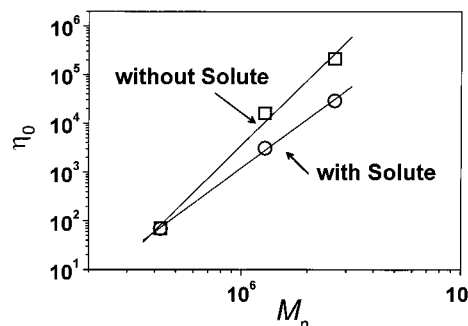


Figure 6. Change of the viscosity of a 1 wt % synthetic HA solution with different molecular weight upon addition of the reactants Rubpy and FC: with (circle) and without (square) solutes as reactants.

This can be attributed to Coulombic interactions with the glucuronic acid groups of HA. It has been known for some time,²⁵ that 2-fold positively charged ions such as Cu²⁺ bind to the HA chain. This leads to the breaking of hydrogen bonds and therefore to a local breakdown of the HA structure. Nevertheless the viscosity remains fairly high.

Fluorescence Measurements. The analysis of the fluorescence decay curves of the sensitizer Rubpy in the presence of the quencher FC shows that time-independent intrinsic quenching rate constants $k_{q,0}$ can be obtained at short times. Their values, given in Table 3, decrease with increasing concentration of the polymer, but are nearly independent of the molecular weight of HA. At longer times, the quenching rate constants were found to be time-dependent. This behavior was described by a polynomial expansion according to eq 6. By comparison with the terms of a cumulant expansion derived from random walk theory, the absolute values of the parameters A_{1-3} can be related to the diffusion constant. Their absolute values also decrease with increasing concentration of the polymer, but are within their error limits independent of the molecular weight of HA (Figure 4). The mean diffusion rates in aqueous solution of the polymer, given by the parameter A_1 , are always larger than the corresponding intrinsic quenching rates $k_{q,0}$. This indicates, that the latter are reaction-controlled. Therefore, the electron transfer process itself seems to be slightly suppressed with increasing concentration of HA. This might be due to a slow of relaxation processes in the solution, leading to a decrease in $k(a)$ in eq 7.

Given that the viscosity of the HA solution in our experiments was varied over 5 orders of magnitude, a large effect on the rate constant for the diffusion-controlled electron-transfer reaction 2 was expected. Surprisingly, it was found that the effect is relatively small. The total decrease of the intrinsic and diffusional quenching rate constants in highly viscous HA solutions was smaller than 20% compared to the value, obtained

in the buffer solution. This result indicates that besides the high viscosity of the bulk solution, the microviscosity inside the aqueous pseudophase remains comparatively small. Nevertheless, the diffusion of the highly negatively charged FC ion is retarded by the HA network. The extent of this suppression rises with increasing concentration but only to a negligible extent with increasing molecular weight. This is also supported by the systematic increase of the lifetime of the sensitizer Rubpy with rising concentration of the polymer, which can be explained by retardation of the quenching of the MLCT state of the ruthenium complex by oxygen.

Comparison with Animal HA. In our previous work,¹⁴ we used the Infelta–Tachiya model to describe the luminescence decay of Rubpy in the presence of the quencher HA. To compare these data with the results of this paper, we explain in the following section the relationship between the Infelta–Tachiya model and the model used in this work. The Infelta–Tachiya model in its simplified form is given by eq 12, where $[Q]$, $[M]$,

$$I = I_0 \exp\left(-\frac{t}{\tau_0} + \bar{n}(\exp(-K_q t) - 1)\right) \quad (12)$$

K_q , and $\bar{n} = [Q]/[M]$ are the concentrations of the quencher and the water microdomains, the first-order quenching constant, and the average number of quencher molecules per microdroplet, respectively. The other symbols have their usual meaning. By inserting eq 12 into eq 4, the time-dependent quenching rate constant can be expressed by eq 13.

$$k_q(t) = \frac{1}{[Q]t} \bar{n}(\exp(-K_q t) - 1) \quad (13)$$

By expansion of the exponent into a Taylor series, it can be shown that eq 12 is equivalent to eq 5 with the parameters A_{1-3} given by eq 14. Although in principle

$$\begin{aligned} A_1 &= \frac{K_q}{[M]} \\ A_2 &= \frac{K_q^2}{[M]} \\ A_3 &= \frac{K_q^3}{[M]} \end{aligned} \quad (14)$$

it is possible to calculate the parameters A_{1-3} from the data given in ref 14 by using eq 14, the error in k_q' and $[M]$ leads to large uncertainty in the higher order values A_2 and A_3 . In agreement with the trend found in this work, the A_1 values decrease slightly with increasing concentration of the polymer.

To clarify this effect, further experiments with HACC were carried out and the results are given in Table 4 and Figure 3. Both the intrinsic quenching rate constants and the diffusion parameters start to decrease at a HA concentration of about 1.0–1.5 wt % in agreement with the structural switch found in animal HA as reported in our previous paper.¹⁴ However, this transition was not found for the synthetic HA samples, again indicating significant structural differences between HA from both sources.

From the measurement of polydispersity for these samples shown in the Experimental Section, no remarkable difference between these two sources was obtained.

Moreover, Figure 5 shows that the zero shear viscosity depends on the concentration in a similar power law for these two kinds. Different from these macroscopic observables, however, the photochemical kinetics and related parameters ($k_{q,0}$, A_i) seem rather sensitive to the source of HA. While the difference in stereochemistry of these HAs may also cause this contrast, small amounts of contaminations such as polypeptide and/or similar kinds of sugars should also affect the present photochemical reaction. The molecular weight is controlled on the stage of the same biosynthesis and HAM0.3–HAM2 are purified through a common method. The present experiments shows synthetic HAs are more suitable to examine the molecular weight dependence of HA solution.

Conclusion

The quenching of electronically excited Rubpy by FC, which was found to occur by direct electron transfer at short times and by a diffusional mechanism at longer time scales provides useful information about the mobility and reactivity of charged reactants in HA solution compared to a homogeneous buffer solution. By variation of the viscosity of the HA solution over 5 orders of magnitude, the rate constants of both quenching processes were found to decrease by about 20%. The main factor, controlling the reaction and diffusion rates is the polymer concentration. In contrast, the increase of the molecular weight of the polymer, which has a comparable effect on the solution viscosity as the increase of the polymer concentration, has only a negligible effect on the rate constants. It was also found that the source of HA provides serious effects on these photochemical properties, which reflects the microscopic structure of HA solution and which is sensitive to the existence of small amount of impurity. Series of HAM satisfactorily provides fair experimental condition to discuss the size (molecular weight) dependence of HA in the present photochemical approach.

Acknowledgment. We thank Dr. Teruzo Miyoshi of Denki Kagaku Kogyo Co. Ltd. for providing us their HA samples. We are also grateful to Mr. Yasufumi Takahashi of Chugai Pharmaceutical Co. Ltd. for his continuous discussion and encouragement throughout the research. This study is partly supported by Grants-in-Aid Nos. 09555026 and 10640506 from the Japanese Ministry of Education, Science, Sports, and Culture.

References and Notes

- (1) Sicińska, W.; Adams, B.; Lerner, L. *Carbohydr. Res.* **1993**, *242*, 29.
- (2) Holmbeck, S. M. A.; Petillo, P. A.; Lerner, L. E. *Biochemistry* **1994**, *33*, 14246.
- (3) Lee, S. A.; Myers, L. C.; Powell, J. W.; Suleski, T. J.; Rupprecht, A. *J. Biomol. Struct. Dyn.* **1993**, *11*, 191.
- (4) Scott, J. E. In *The biology of hyaluronan*; Wiley-Interscience: Chichester, England, 1989; pp 6–20.
- (5) Mikelsaar, R. H.; Scott, J. E. *Glycoconj. J.* **1994**, *11*, 65.
- (6) Perkins, S. J.; Nealis, A. S.; Dunham, D. G.; Hardingham, T. E.; Muir, I. H. *Biochem. J.* **1992**, *285*, 263.
- (7) Staskus, P. W.; Johnson, W. C. *Biochemistry* **1988**, *27*, 1522.
- (8) Scott, J. E.; Cummings, C.; Brass, A.; Chen, Y. *Biochem. J.* **1991**, *274*, 699.
- (9) Fouissac, E.; Milas, M.; Rinaudo, M. *Macromolecules* **1993**, *26*, 6945.
- (10) Kobayashi, Y.; Okamoto, A.; Nishinari, K. *Biorheology* **1994**, *31*, 235.
- (11) Roure, I.; Rinaudo, M.; Milas, M. *Ber. Bunsen-Ges. Phys. Chem.* **1996**, *100*, 703.

- (12) Lapčik Jr., L.; Lapčik, L.; De Smedt, S.; Demeester, J.; Chabreček, P. *Chem. Rev.* **1998**, *98*, 2664.
- (13) Lianos, P.; Modes, S.; Staikos, G.; Brown, W. *Langmuir* **1992**, *8*, 1054.
- (14) Kluge, T.; Masuda, A.; Yamashita, K.; Ushida, K. *Photochem. Photobiol.* **1998**, *68*, 771.
- (15) Ghosh, S.; Li, X.; Reed, C. E.; Reed, W. F. *Biopolymers* **1990**, *30*, 1101.
- (16) Morris, E. R. *Carbohydr. Polym.* **1990**, *13*, 85.
- (17) Pisárčik, M.; Bakoš, D.; Čeppan, M. *Colloids Surf.* **1995**, *97*, 197.
- (18) Infelta, P. P.; Grätzel, M.; Thomas, J. K. *J. Phys. Chem.* **1974**, *78*, 190.
- (19) Tachiya, M. *Chem. Phys. Lett.* **1975**, *33*, 289.
- (20) Almgren, M.; Löfroth, J.-E.; van Stam, J. *J. Phys. Chem.* **1986**, *90*, 4431.
- (21) Inokuti, M.; Hirayama, F. *J. Chem. Phys.* **1965**, *64*, 1978.
- (22) Blumen, A. *J. Chem. Phys.* **1980**, *72*, 2632.
- (23) Lianos, P.; Argyrakís, P. *J. Phys. Chem.* **1994**, *98*, 7278.
- (24) Ahn, J.; Kopelmann, R.; Argyrakís, P. *J. Chem. Phys.* **1999**, *110*, 2117 and references therein.
- (25) Lapčik, L., Jr.; Dammer, C.; Valko, M. *Colloid Polym. Sci.* **1992**, *270*, 1049.

MA990649S